Published in final edited form as:
Brain Res. 2007 May 4; 1144: 209–218. doi:10.1016/j.brainres.2007.01.134.

Metabolic and Behavioral Deficits Following a Routine Surgical Procedure in Rats

David B. Frumberg[1,2], **Marion S. Fernando**[2], **Dianne E. Lee**[2], **Anat Biegon**[2], and **Wynne K. Schiffer**[2,*]

[1]Cornell University, Ithaca NY, 14853

[2]Medical Department, Brookhaven National Laboratory, Upton NY 11973

Abstract

To test the hypothesis that functional metabolic deficits observed following surgical brain injury are associated with changes in cognitive performance in rodents, we performed serial imaging studies in parallel with behavioral measures in control animals and in animals with surgical implants. Memory function was assessed using the novel object recognition (NOR) test, administered 3 days prior to and 3, 7, 14, and 56 days after surgery. At each time point, general locomotion was also measured. Metabolic imaging with ^{18}F-fluorodeoxyglucose ([^{18}F]FDG) occurred 28 and 58 days after surgery. Animals with surgical implants performed significantly worse on tests of object recognition, while general locomotion was unaffected by the implant. There was a significant decrease in glucose uptake after surgery in most of the hemisphere ipsilateral to the implant relative to the contralateral hemisphere. At both time points, the most significant metabolic deficits occurred in the primary motor cortex (-25%; $p<0.001$), sensory cortex (-15%, $p<0.001$) and frontal cortex (-12%; $p<0.001$). Ipsilateral areas further from the site of insertion became progressively worse, including the sensory cortex, dorsal striatum and thalamus. This data was supported by a voxel-based analysis of the PET data, which revealed again a unilateral decrease in [^{18}F]FDG uptake that extended throughout the ipsilateral cortex and persisted for the duration of the 58-day study. Probe implantation in the striatum results in a widespread and long lasting decline in cortical glucose metabolism together with a persistent, injury-related deficit in the performance of a cognitive (object recognition) task in rats.

Keywords

Glucose metabolism; brain injury; behavior; surgery; microdialysis; functional neuroimaging; parametric mapping

1. Introduction

In human subjects as well as in animal models, cognitive deficits are an extremely common finding in the aftermath of surgical, traumatic and ischemic brain injuries [10,12,14,19, 22-25]. Thousands of clinical neurosurgical procedures ranging from insertion of biopsy

*Corresponding Author: Wynne K. Schiffer, Assistant Scientist, Brookhaven National Laboratory, Building #555, Upton, NY 11973, e-mail: E-mail: wynne@bnl.gov, phone: (631) 344-6269, fax: (586) 279-6268.

needles, shunts, catheters and electrodes to large resections and ablations are performed every day. In experimental animals, surgical procedures such as cannulation, electrode placement and microdialysis probe implants are performed routinely in studies of brain organization and function. Studies in our laboratory and others have shown that following these routine surgical procedures, animals undergo dramatic short-term and long-term neurochemical and metabolic changes [5,34,39,41,46].

Unlike injury-induced depressions that eventually recover in a matter of days or weeks, our previous observations of a persistent decrease in glucose metabolic rate as many as 25 days after the implant points toward a more enduring metabolic depression with a surgical implant. At a cellular level, it has been shown that activated, proliferating microglia appear around the implant site as early as 1-day post implantation [18,21,42]. These activated microglia are thought to gradually diminish both excess fluid and cellular debris 6 – 8 days after the implant, although necrotic tissue has been observed up to 42 days later [41,44]. At later time points, typical inflammatory cells or hemorrhaging has not been observed [47], while others have documented neuronal cell loss and macrophages up to 112 days after the implant [6,41,42, 44]. As a testament to the transitory nature of this mechanically induced wound healing response, electrode tracks could not be found in animals after several months when the electrode was inserted and quickly removed [6,13,35,47]. We have shown a similar effect with FDG, since glucose metabolism returned to normal levels within seven days if the microdialysis probe was inserted and immediately removed [39]. Taken together, it appears that injury alone produces a more transient metabolic response while the implant appears to induce a more enduring brain tissue response.

Specifically, brain energy metabolism after injury fluctuates such that immediately after injury, a hyperactivated state lasting only 30 minutes (in rats) to a few hours (in humans) is followed by a metabolic depression lasting from 5-10 or 30 days in rats or humans, respectively [4,27, 30,46]. We have recently used serial small animal PET imaging to show a profound, persistent metabolic decline following microdialysis cannula implant that began as early as 2.0 hrs after the surgery, was at its lowest point 48 hrs after the surgery and persisted for the duration of the experiment, 25 days [39]. In a related series of studies, we have also used autoradiography to show that mice subjected to closed head injury undergo dynamic changes in glutamate NMDA receptor activation and availability [5]. These studies demonstrated a transient increase in NMDA receptor function within the first hour of injury followed by long lasting decrease (over 7 days).

Since cognitive impairments are extremely common and often long lasting after brain injuries in humans [26], we sought to examine the presence and time course of cognitive deficits following surgical brain injury in rodents. In animal models, long lasting cognitive deficits are observed not only after severe brain injury [10] but also after moderate [33] and even mild concussions which do not involve appreciable neuronal cell loss [48]. More recent studies in animals are beginning to report significant inflammation and neurodegeration linked to minor surgery such as electrode implanatation [34], although to our knowledge the cognitive effects of a microdialysis probe cannulation have not been documented.

Many cortical brain regions are pivotal to the formation of memories and brain plasticity [3, 7,29] and intracranial surgery usually involves cortical regions even if the target is subcortical. For example, a surgical implant targeting the striatum passes through the motor and sensory cortices of the rat, and we have shown that these areas as well as distal cortical areas show a persistent metabolic decline long after the cannulation. It follows that if an intracranial implant targeting the striatum damages cortical regions, it may also impact memory function. The striatum has also been implicated in learning and memory, adding to the potential cognitive impact of striatal implants [8,9,36]. We therefore sought to extend our previous findings of

metabolic functional deficits by assessing working memory function and general locomotion in rats following a unilateral microdialysis cannulation targeting the striatum. While our previous study characterized metabolic deficits immediately following the injury (from 2 hours to 25 days), here we have extended these observations by scanning animals with [^{18}F]FDG at 28 and 58 days after the procedure. Thus, while the overarching goal of these experiments was to determine whether or not the probe induced a measurable change in cognition in these animals, [^{18}F]FDG scans were performed to ensure that the hypometabolic state described in our previous report not only existed in these animals, but persisted for the duration of the 56 day behavioral experiment. Our results show that rats with chronic implants have deficits in a working memory task as well as widespread decreases in glucose uptake in brain regions ipsilateral to the implanted probe.

2. Results

Twenty-two animals began the study by performing the pre-surgical NOR. After this eleven of these animals received surgical implants and eleven were anesthetized as control animals. Two animals died from the initial anesthesia, leaving 20 animals. Not all of the animals were scanned with [^{18}F]FDG. Of these animals, fourteen were scanned with [^{18}F]FDG at 28 days after the surgery (control n = 7, surgical n = 7). These same animals were scanned 58 days after the surgery, although one of the implanted animals had to be euthanized. Only a subset of animals could be scanned because the maximum number of animals that can receive [^{18}F]FDG in an experimental day varies as a function of radiotracer delivery and scanner availability. To be safe and to take into account these factors, we planned to scan 14 animals per day. Thus, although 10 controls and 8 implanted rats had pre-surgical testing on the NOR and also were tested in the NOR at each of the post-surgical tests (i.e., at 3, 7, 14 and 56 days). Seven rats in each group were scanned 28 days after the surgery and all but one of these animals had a second PET scan at day 58 post-surgery. In other words, 7 control rats and 6 implanted rats had both the pre-and post-surgical behavioral assessments and the FDG scans. Scanning times were chosen based on our previously published report of metabolic deficits as late as 25 days after the surgical implant. To extend these earlier results and to ensure the presence of the metabolic deficit, we scanned animals at 28 days and again two days following the culmination of the behavioral portion of these experiments.

2.1 NOR and Locomotion

The outcome measure for the NOR experiments is proportional time spent with a novel object. In the familiarization phase, animals spent equal time investigating the identical objects. Test data is summarized in Figure 1 for both control and surgically implanted animals. The proportional time spent at novel and familiar objects was not significantly different between groups in the pretest (anesthesia controls spent 69% of their time with the novel object while surgically implanted animals spent 61% of their time with the novel object, p=0.078), indicating that rats in both experimental conditions readily discriminated the novel object prior to the surgical or sham procedure. On the pre-surgical data, a two factor (Group X Object) ANOVA indicated there was no significant effect of Group (P=1.0) and no interaction between Group and Object ($F_{[1,1]}$=3.39, P=0.08). Therefore, this data was combined in Figure 1. As shown in this figure, the surgical implant impaired retention performance of rats. Control animals continued to spend significantly more time with the novel object as the trials continued, while surgically implanted animals did not. If only those animals which were scanned and completed all NOR test days (e.g. animals that did not lose their surgical implants in the course of the study) are considered, the proportional time spent investigating the novel object is the same as if both scanned and unscanned animals are considered. Table 2 presents the behavioral results from only those animals that were scanned. Two-way ANOVA of this dataset indicates a significant effect of Day (with a dependent variable of proportional time spent with novel

object; F=7.71, P<0.001) and of Group (F=14.9, P=0.001) but no interaction between the two F=0.38, P=0.8). This allows a more accurate correlation with changes in regional [^{18}F]FDG uptake as well as facilitates a repeated measures statistical analysis. Two way repeated measures ANOVA for exploration time of the novel object revealed a significant main effect of the surgery (control versus cannulated animals; $F_{[1,12]} = 15.02$, $P = 0.002$) and the post-surgical day ($F_{[4,12]} = 7.08$, $P < 0.001$) but no interaction between surgical implant and day following the procedure ($F_{[4,12]} = 0.44$, $P = 0.78$). Post hoc Bonferroni t-test indicated that the time exploring the novel object on the presurgical test day significantly differed from both the 14-day test (t=2.86, p=0.039) and from the 56-day test (t=3.20, p=0.02). Control animals did not differ in time exploring the novel object between testing days ($F_{[7,4]}$=2.0, P = 0.118).

Distance traveled during the test phase was compiled to yield an index of locomotion. There were no significant differences between the two groups at any time point. Two-way repeated measures ANOVA for distance traveled (in millimeters) demonstrated no main effect of Day (pre-surgical, 3, 7, 14 and 56 days later) or Group (control vs. surgical) and no interaction between the two factors ($F_{[7,4]}$=0.56, P=0.69). There was no correlation between the distance traveled during the test and the time spent at the novel object (R^2=0.093).

2.2 [^{18}F]FDG microPET results

The changes in [^{18}F]FDG uptake in rats with a surgical implant compared to controls are displayed in several ways. First, they are shown as mean [^{18}F]FDG uptake images (Figure 2), where scans that were both spatially and globally normalized were averaged by group. These mean images show the difference in FDG uptake in control animals (Figure 2b) versus animals with cannulations (Figure 2c and d). Second, regional decreases in surgically implanted animals compared to controls 28 days after the procedure are displayed on a representative three-dimensional brain model to facilitate visualization of spatial relations ('glass-brain' view; Figure 3). It is evident from this figure that the extent of voxels which are significantly different from control animals is focused around the site of probe insertion. Third, both increases and decreases at 58 days after the procedure are shown as a color-coded statistical t-map (Figure 4) superimposed on a three-dimensional atlas of the rat brain [40]. Compared to the glass-brain view presented in Figure 3, it appears that the extent of voxels which are significantly decreased compared to control has increased to incorporate much of the ipsilateral hemisphere. Finally, Table 1 lists the percentage change between hemispheres with the ROI-based analysis. Our previous studies demonstrated that at later time points, [^{18}F]FDG uptake contralateral to the probe is not significantly different from pre-scan levels [39]. Therefore, statistical comparisons were made using the proportional difference between hemispheres. Three way ANOVA for percent asymmetry with factors of Group, Brain Region and Time revealed a significant main effect for Group ($F_{[1,264]} = 154.96$, $P < 0.001$) and Region ($F_{[10,264]} = 7.46$, $P < 0.001$) but no main effect for Time ($F_{[1,264]} = 0.19$, $P = 0.657$). A significant interaction occurred between Group and Brain Region ($F_{[1,11]} = 11.96$, $P < 0.001$), where the most impacted regions were the primary motor cortex followed by the primary sensory and frontal cortices ($F_{[3,11]}$=45.1, P<0.001). Two-way repeated measures analysis of percent asymmetry data from only cannulated animals that completed both scans were performed for each region, where factors were Group and Time. None of the regions were significantly different between the scan 28 days and 58 days after the procedure. Thus, the decrease in metabolism did not recover, nor did it significantly decline. The hippocampus, colliculi and cerebellum appear to be relatively spared, since the proportional difference between hemispheres was not different from controls in these regions.

According to the voxel-based analysis, which is not based on hemispheric differences but based on voxels which are significantly different between control and surgically implanted animals, several additional regions showed marked effects of the surgical implant. In cannulated animals

28 days after surgery, the statistical parametric mapping analysis identified two regions (clusters) in which there was a significantly lower [^{18}F]FDG uptake as compared with that for the control group (Figure 3). The area revealing the most significant difference between the groups is located on the border of the ipsilateral motor and sensory cortices, the coordinates of which are given in Figure 3. The center of the second significant cluster of deactivation is in the striatum, at 2.8, 1.4, -5.8. There were no significant increases in this comparison, however at 58 days the voxel-based analysis indicated increased activity in the region around the contralateral amygdala (-6.0, -1.8, -9.2; x,y,z), contralateral insular and perirhinal regions (-4.4, 1.6, -7.0; x,y,z) and contralateral caudate/putamen (-3.8, 1.2, -5.1; x,y,z). Significant decreases at this time point were contained within the cortex (Figure 4).

3. Discussion

Implantation of microdialysis cannulas, probes and shunts are procedures used in a number of experimental protocols. In humans, similar procedures are used for surgical interventions such as implantation of intracranial pressure monitors, microdialysis probes, shunts and stimulating electrodes. In these procedures, the implanted object remains in the brain for periods ranging from a few days to weeks, months or years. Previously, we have shown that intracerebral microdialysis implants cause a lasting decline in glucose metabolism for as long as twenty five days after the surgery [39]. In this report, there were no alterations in the rate constants governing radiotracer delivery to the brain (K1) or phosphorylation by hexokinase (k3), however there was a significantly more rapid dephosphorylation (k4). Related experiments used ^{3}H-PK11195 in surgically implanted animals to show two-fold increases in peripheral benzodiazepine receptor activation in brain regions close to the site of the implant (frontal cortex, anterior cingulate), and increases of 30-50 percent were observed distally in the dentate gyrus and temporal cortex [43]. Here we extend these findings to show that the decline in [^{18}F]FDG uptake persists to 58 days following implant and is associated with a significant and equally persistent cognitive impairment in these animals.

To our knowledge, there have been no studies of the impact of a routine microdialysis surgery on cognitive performance in animals. *In vivo* microdialysis is widely used because it provides on-line measurements of neurochemical flux in behaving animals. Our previous observations of the metabolic decline in animals following this routine surgical procedure were not accompanied by any behavioral measurements, although casual observations did not support any changes in locomotor behavior. In the present experiment, there were no apparent differences in general locomotion between animals that had probes and animals that did not, although a more sensitive measure may yield information on ipsilateral and contralateral behavioral asymmetries. What we do observe however, is that when challenged with a cognitive task, animals who have been anesthetized and had microdialysis probes inserted perform very differently from animals that have just been anesthetized (Figure 1). Further, these animals show a profound decrease in glucose metabolism that extends far from the site of cannula insertion. Performance differences in the working memory task were observed between animals that received routine microdialysis cannulations and animals that were anesthetized as non-surgical controls. These cognitive changes are consistent with the probe-induced decrease in glucose metabolic rate observed previously, and persist in parallel with changes in FDG uptake in the present experiments.

Unequivocal conclusions cannot be drawn without further investigation of the effect of surgical implants on cognition and behavior using more sensitive measures. Working memory impairment reported here is only one potential explanation for the behavioral deficits observed in cannulated animals. It is important to note that the NOR task, as it was administered, can not differentiate between sensory or perceptual problems versus retrieval impairments. Deficits observed here may only be sensory in nature; that is, these animals may be unable to store the

memory of their prior experience with the objects in the first place. Presumably, this is due to the implant targeting the striatum and passing through the cortex between the sensorimotor and motor cortices. Thus, memory impairment per se may only be one potential explanation for the behavioral differences in cannulated animals versus controls. Further studies are needed to examine the effects of a surgical implant in comparable tasks that permit an evaluation of ipsilateral and contralateral behavioral asymmetries, coordination and other sensory/attentional deficits.

Studies of brain energy metabolism after human and rodent brain injury demonstrate dynamic changes occurring during the acute period after injury, such that a hypermetabolic state lasting only 30 minutes (in rats) to a few hours (in humans) is followed by a profound depression lasting 5-10 to 30 days in rats and humans, respectively [27,30,46]. Along the same time course, we have recently shown that NMDA glutamate receptors in mice subjected to closed head injury undergo dynamic changes in activation and availability [5], with a transient activation (less than 1 hour) followed by long lasting decrease (over seven days) in receptor function and availability. At later time points, we have shown that the metabolic deficit is most likely related to the dephosphorylation of FDG. There were no alterations in the rate constants governing radiotracer delivery to the brain or phosphorylation by hexokinase, however there was a significantly more rapid dephosphorylation. Thus, enduring metabolic and cognitive deficits observed here may lead to more chronic changes in NMDA receptor function and availability.

In these studies as well as in our previous experiments, animals with the surgical implants had little or no recovery of metabolic function while also showing no recovery of behavioral function. This distinguishes the present studies from other investigations of brain injury, where acute insults to the brain were shown to result in widespread metabolic deficits that improved with time [4,11,30,46]. In brain lesion models, the period of post-injury metabolic depression has been shown to correlate with the duration of behavioral deficits [11,20,45]. Resolution of these model injuries, either spontaneously or through pharmacological treatment, is thought to play a significant role in the recovery of behavioral function [17]. We have previously shown that the hypometabolism recovers to control levels within 7 days if the implant is inserted and immediately removed [39]. It thus appears that the prolonged and persistent decrease in brain metabolism is associated with the implant, since without it this procedure produces an effect that recovers over time. Given the lack of recovery and persisting deficit in behavioral performance, we found no correlation between the degree or extent of the metabolic decline to the severity of behavioral deficits. This may also have been because the present experiments measured basal, resting glucose metabolism in injured animals, instead of measuring metabolism in an activated injured brain. Our measures of cerebral metabolism at rest did not asses the capacity of the injured brain to utilize metabolic energy in times of increased demand, such as during task performance.

An alternative and perhaps more sensitive strategy would be to measure [^{18}F]FDG uptake as the animals are performing the NOR task or even a more sensitive measure of asymmetry or coordination. It is likely the pattern of brain activations captured during the baseline state differs from the activated state, and thus may reveal a different pattern of functional deficits in animals with surgical implants and/or injuries. Such studies may reveal alterations in glucose metabolism during activated states that may not be otherwise detected. Nevertheless, it appears that a relatively small brain implant (300 μm probe) produces a widespread ipsilateral suppression of brain glucose metabolism and a dramatic decrease in working memory performance.

Comparisons of ipsilateral to contralateral hemispheres are predicated on our previous fully quantitative microPET findings, in which an identical surgery did not increase the rate of glucose metabolism in the contralateral hemisphere [39]. Here, the parametric, voxel-based

analysis provides an efficient way of assessing regional increases in the whole brain. According to the parametric map, there appear to be several areas of significant increase in the contralateral hemisphere at 58, but not at 28, days after the procedure (Figure 4). This may represent some reorganization in the face of prolonged damage caused by the implant. It is also important to note that the increases in the present study were only observed in the SPM analysis and two of the regions (perirhinal cortex and amygdala) are not included in our ROI template. Nevertheless, the SPM detected several regions of contralateral activation that were not evident in the ROI analysis. On the one hand, it is well known that the size and shape of regions chosen for an ROI analysis and the number of planes of data on which they are placed may introduce a subjective error. If regional brain activations lie partially outside the defined ROI, a failure to detect a significant activation may result. However if regions of brain activation are substantially smaller than the defined ROI, significant activation may be missed when active signal is averaged with the surrounding background within the ROI.

The study of rodent models has proven to be critical for the understanding of anatomical, biochemical, and molecular responses to brain injury or insults, as well as to provide the means to test novel therapies and assess the consequences of routine interventions. The use of PET in rodent models of CNS plasticity allows for powerful *in vivo* observations and within-animal designs. The application of parametric mapping approaches strengthens these strategies and provides an outcome measure that can be readily translated from animal models to human diseases.

4. Experimental Procedure

4.1 Experimental Design

Our study employed 16 adult male Sprague-Dawley rats (250-300g, ~55 days of age, Taconic Farms, Long Island, NY) and was approved by the Institutional Animal Care and Use Committee (IACUC).

All animals were given preliminary novel object recognition (NOR) tests to determine baseline (pre-surgical) performance [15]. Animals were then divided into two groups where one group received anesthesia only and the other received anesthesia during which a microdialysis cannula was implanted in the right striatum. Both groups received behavioral tests at 3, 7, 14, and 56 days after the procedure and microPET [^{18}F]FDG scans at 28 and 58 days.

4.2 Surgical Implantation

All animals were anesthetized with intra-peritoneal (i.p.) injections of 1.5 mL chloral hydrate (8%). Intracerebral guide cannulae and stylets (BAS, West Lafayette, IN; 300 μm outer diameter) were inserted into the right striatum using established procedures [37,38]. The coordinates for the striatum were obtained from the Paxinos and Watson stereotaxic atlas: 0.5 mm anterior and 2.5 mm lateral to bregma, and 6.0 mm below the surface of the brain [32]. Guide cannulae were secured with dental acrylic, which was affixed to the skull by four nylon bone screws. Once solid and in place, the stylet was removed from the guide cannula, trimmed down using a Dremel Moto-Tool sander, and reinserted. This prevented animals from catching their caps on their cages and/or scratching them off during the two-month study. All animals received antibiotic immediately following the surgery (0.1 mL Baytril given intramuscularly).

4.3 Behavioral Measures: Novel Object Recognition (NOR) and Locomotion

The object recognition test was similar to that originally described by Ennaceur and Delacour [15]. The testing arena was an opaque, plastic rectangle measuring 65 × 45 × 45cm. Two objects were placed at one end of the arena floor with sufficient space on all sides for rats to survey each side of each object. Objects were affixed to the arena floor using Velcro. Pairs of objects

were of the same material but varied in shape and color. Objects were sized to be roughly the same surface area as the animals. Before each phase of the NOR, objects and the chamber were rinsed with a 10% ethanol solution.

At the start of each testing day, animals were placed in the test room for at least 45 minutes to adjust to conditions. The test room was fully lit with overhead fluorescent lights, and tests commenced in the evening to alleviate some lethargy due to the nocturnal nature of rats. Each experimental day consisted of two phases – the familiarization phase and the testing phase. These two phases were separated by a four-hour delay. In the familiarization phase, two identical objects were placed in the arena. Rats were placed in the arena and allowed to explore the identical objects for 10 minutes, after which they were removed and returned to their home cages for four (4) hours. In the testing phase, one of the objects was replaced by a new, novel object. Of the two objects, the familiar object used in this testing phase was selected randomly prior to the start of each set of recognition experiments. The position of the novel object (left or right placement of the object) was also randomized during the different test sessions. During the test session, rats were placed in the arena and allowed to explore the novel and familiar objects for five minutes.

The animals and cages were monitored by a video surveillance camera mounted on the ceiling. Cumulative time spent by the rats at each of the objects during the 5 minute test was scored from the digital video. Data were evaluated manually by quantitating the time in seconds that each rat spent investigating each object, with an investigation being defined as seconds spent sniffing an object or climbing on its sides. The time spent at each of the objects was recorded for both phases, and only the time spent exploring objects was used to calculate the duration at each (e.g. time at novel/time at novel + time at familiar object). The basic measure is the percent of the investigation time spent by each animal at each object during a five minute testing period. This measure was first described as the discrimination index previously reported by Ennaceur [16] calculated as the difference in time exploring the novel and familiar object. The discrimination index is expressed as the ratio of the total time spent exploring both objects, making it possible to adjust for any difference in total exploration time [16,31].

Video data was also analyzed for total locomotion using TopScan 1.0 (CleverSys, Inc., Reston, VA). For this measure, distance traveled (in mm) by each animal was recorded for both the familiarization and testing phases and the locomotion data for the test session was compared to the proportional time spent at the novel object during this session. Significant differences were assessed on a test-by-test basis by comparing the proportional time spent at novel versus familiar objects with a Student's t-test.

4.4 [^{18}F]FDG microPET Scans

On the day of each microPET study, fully conscious animals were injected i.p. with 500-700 μCi [^{18}F]FDG in their home cages. Using a time course established from previous studies, uptake occurred for 50 minutes following radiotracer injection [39]. After 50 min, animals were lightly anesthetized with chloral hydrate (8%), positioned in a nylon stereotaxic frame (Kopf Instruments, Tujunga, CA) and underwent a 10 minute microPET acquisition. One blood sample was taken at the end of the scan, after the tail was placed under a heat-lamp for several minutes. This final sample was split and used (1) with a glucometer to assess whole blood glucose levels and (2) with a well counter to measure the amount of 18F in the blood. These values were used to normalize [^{18}F]FDG data.

Emission data were collected using a first-generation microPET R4 (CTI/Siemens, Knoxville, TN), housed in a temperature controlled suite. The R4 tomograph has a transaxial resolution of 2.0 mm full width at half maximum (FWHM) in a 12 cm animal port, with an image field of view of 11.5 cm. Animals were placed in a prone position using a nylon stereotaxic head

holding device manufactured by Kopf Instruments (Tujunga, California, USA). All animals were placed in the center of the field of view. All microPET frames included subtraction of random coincidences collected in a delayed time window. 3D sinograms were converted into 2D sinograms before image reconstruction. This was done with the process of Fourier rebinning. After Fourier rebinning, images were reconstructed by 2D-filtered back projection using a ramp filter with cutoff at one-half the Nyquist criteria (maximum sampling frequency). Data were corrected for photon scatter using a method previously established in our laboratory [1]. At the time of these studies, the measured attenuation correction method available for this system used a 68Ge point source and contributed a degree of noise to the transmission scans [1]. Therefore, attenuation correction was not applied. Sinograms were first reconstructed using the manufacturer's filtered back projection (FBP) software. The volumetric resolution using this method is ~5.0 μl at the center of the field of view on the basis of the 10-ns timing window and is less than ~14 μl within a 1.0 cm radius. A complete performance evaluation of the scanner has been done by Knoess et al. [28]. Scatter-corrected sinograms were also reconstructed using an iterative maximum likelihood maximization estimation (MLEM) algorithm. The image pixel size in FBP reconstructed images was 0.85 mm transaxially with a 1.21 mm slice thickness, and MLEM reconstructed images had a pixel size of 0.4 × 0.4 × 1.21 mm (x, y, z).

4.5 Image Analysis

A requirement for whole-brain analysis is that the images of different brains must be spatially normalized into a standard space, which we identified as Paxinos and Watson [32] stereotaxic space. We first chose one control [^{18}F]FDG scan with a high degree of symmetry, alignment and freedom from obvious artifacts. Using the SPM software, this reference scan was smoothed with a Gaussian kernel of full width at half maximum (FWHM) of 3 mm (three times the voxel dimensions), so that artifacts from outstanding features of the brain would not bias the normalization. Next, each control rat brain was co-registered and spatially normalized to the smoothed reference brain. Spatial normalization consisted of a 12-parameter affine transformation, followed by a non-linear spatial normalization using the low-frequency basis functions of the three dimensional discrete cosine transform (6 × 8 × 5 in each direction) plus a linear intensity transformation [2]. This process was implemented in SPM, where the intensities from the original images were mapped into normalized images. In the warping procedure for creating the normalized images, the following SPM options were used: heavy regularization to penalize large deformations, 12 iterations and trilinear interpolation. The images of the reference brain and remaining normalized brains (all unsmoothed) were averaged to create a mean image. This mean image was divided by the average pixel value to give a ratio-to-whole brain image and smoothed with a 6 mm FWHM Gaussian kernel. The smoothed brain was then coregistered to an MRI template [40] and became the [^{18}F]FDG template brain to which all scans were spatially normalized. For each [^{18}F]FDG scan, the radioactivity distribution was divided by the mean pixel value to give one scan where the pixel values were normalized to match the template in addition to the original radioactivity distribution.

A Region of Interest (ROI) template was developed in PMOD based on a digital atlas of the rat brain [40] which was subsequently applied to all spatially normalized microPET data. The ROI template included 10 regions based on a functional atlas of the rat brain [32]; the Frontal/Prelimbic/Cingulate cortex (FrA-PrL-Cg; with the center at ±0.9 mm lateral to bregma, x axis; +1.6 mm anterior to bregma, y axis; -3.1 mm below bregma, z axis), primary motor cortex (M1; ±3.4, +1.3, -3.1 x, y, z), sensory cortex (S1; ±4.3, -0.9, -4.6 x, y, z), auditory/temporal association cortex (temporal, AuTeA; ±5.5, -5.3, -4.6, x, y, z), primary visual cortex (V1-V2; ±3.7, -6.2, -2.0 x, y, z), caudate/putamen (CPu; ±2.2, +0.6, -5.6 x, y, z), thalamus (Thal; ±1.8, -3.2, -6.4 x, y, z), hippocampus (Hippo; ±2.4; -4.2, -4.0 x, y, z), superior colliculi (Colliculi; ±1.7, -8.1, -3.7 x, y, z) and cerebellum (CB; ±1.9, -12.5, -6.0 x, y, z). The mean volume of all ROIs was 0.86 cm^3 and the shapes were elliptical or round. Since the SPM rat atlas template

is in Paxinos and Watson [32] stereotaxic space, the center of all ROIs corresponded to the location of the region in three dimensional coordinate plane (given in parentheses above). This allows a direct comparison with the surgical implant, which is guided by the same coordinate system.

Before statistical analysis, each of the scans were individually smoothed with a Gaussian kernel to reduce the impact of misregistration into template space and to satisfy the assumption of Gaussian random field theory and to improve the signal to noise ratio. These criteria require that smoothness be substantially greater than voxel size. Next, to ensure that only voxels mapping cerebral tissue were included in the analysis, voxels for each brain failing to reach a specified threshold were masked out to eliminate the background and ventricular spaces. We set the default threshold as 80% of the mean voxel value inside the brain (threshold masking). In addition, global differences in the absolute amount of [^{18}F]FDG delivered to the brain were adjusted by scaling the voxel intensities so that the mean intensity for each brain was the same (global normalization).

To examine regional differences in [^{18}F]FDG uptake between the control and surgically implanted scans on a voxel-by-voxel basis, a t-test was performed across groups using the SPM2 software package. Because some animals that were scanned 28 days after the surgery did not survive to the second, 58-day scan, groups were entered separately and comparisons were made based on scan. To do this, separate t-tests were performed on controls and surgically implanted animals from Scan 1 (at 28 days after the anesthesia/surgery), then on controls and surgically implanted animals from Scan 2 (at 28 days after the anesthesia/surgery). Spatially extended statistical results, or SPM t-maps, were used to characterize and present regionally specific effects in the imaging data.

For the ROI analysis of differences between the control and surgically implanted groups, a two-way ANOVA was performed where the factors of brain region and group (4 groups: Control Scan 1 and Scan 2, Surgical Implant Scan 1 and Scan 2) were assessed using the outcome measure of percent difference between hemispheres. This was chosen because we have previously established using fully quantitative microPET and [^{18}F]FDG that at later time points, metabolic rates in the hemisphere contralateral to the implant do not significantly differ from pre-surgical rates measured from the same animals [39]. Post hoc significance was determined using a Bonferroni analysis. The threshold for ROI calculations was set at $P<0.05$ (two-tailed).

Acknowledgments

Supported by National Institutes of Health grant DA15082 and performed under Brookhaven Science Associates contract No. DE-AC02-98CH10886 with the U.S. Department of Energy. We greatly appreciate the efforts of David Alexoff, Colleen Shea, Lisa Muench, Youwen Xu and Drs. Joanna Fowler, Stephen Dewey, Mike Schueller, Paul Vaska, Richard Ferrieri and David Schlyer, and technical assistance from James Anselmini, Steve Howell and Barry Laffler in the BNL Chemistry Department.

References

1. Alexoff DL, Vaska P, Marsteller D, Gerasimov T, Li J, Logan J, Fowler JS, Taintor NB, Thanos PK, Volkow ND. Reproducibility of 11C-raclopride binding in the rat brain measured with the microPET R4: effects of scatter correction and tracer specific activity. J Nucl Med 2003;44:815–22. [PubMed: 12732684]
2. Ashburner J, Friston KJ. Nonlinear spatial normalization using basis functions. Hum Brain Mapp 1999;7:254–66. [PubMed: 10408769]
3. Baker KB, Kim JJ. Effects of stress and hippocampal NMDA receptor antagonism on recognition memory in rats. Learn Mem 2002;9:58–65. [PubMed: 11992016]

4. Bergsneider M, Hovda DA, McArthur DL, Etchepare M, Huang SC, Sehati N, Satz P, Phelps ME, Becker DP. Metabolic recovery following human traumatic brain injury based on FDG-PET: time course and relationship to neurological disability. J Head Trauma Rehabil 2001;16:135–48. [PubMed: 11275575]
5. Biegon A, Fry PA, Paden CM, Alexandrovich A, Tsenter J, Shohami E. Dynamic changes in N-methyl-D-aspartate receptors after closed head injury in mice: Implications for treatment of neurological and cognitive deficits. Proc Natl Acad Sci U S A 2004;101:5117–22. [PubMed: 15044697]
6. Biran R, Martin DC, Tresco PA. Neuronal cell loss accompanies the brain tissue response to chronically implanted silicon microelectrode arrays. Exp Neurol 2005;195:115–26. [PubMed: 16045910]
7. Broersen LM. Attentional processes and learning and memory in rats: the prefrontal cortex and hippocampus compared. Prog Brain Res 2000;126:79–94. [PubMed: 11105641]
8. Chang Q, Gold PE. Switching memory systems during learning: changes in patterns of brain acetylcholine release in the hippocampus and striatum in rats. J Neurosci 2003;23:3001–5. [PubMed: 12684487]
9. Chang Q, Gold PE. Inactivation of dorsolateral striatum impairs acquisition of response learning in cue-deficient, but not cue-available, conditions. Behav Neurosci 2004;118:383–8. [PubMed: 15113264]
10. Chen M, Bullock R, Graham DI, Frey P, Lowe D, McCulloch J. Evaluation of a competitive NMDA antagonist (D-CPPene) in feline focal cerebral ischemia. Ann Neurol 1991;30:62–70. [PubMed: 1834008]
11. Colle LM, Holmes LJ, Pappius HM. Correlation between behavioral status and cerebral glucose utilization in rats following freezing lesion. Brain Res 1986;397:27–36. [PubMed: 3801863]
12. Courtiere A, Hardouin J, Locatelli V, Turle-Lorenzo N, Amalric M, Vidal F, Hasbroucq T. Selective effects of partial striatal 6-OHDA lesions on information processing in the rat. Eur J Neurosci 2005;21:1973–83. [PubMed: 15869490]
13. Csicsvari J, Henze DA, Jamieson B, Harris KD, Sirota A, Bartho P, Wise KD, Buzsaki G. Massively parallel recording of unit and local field potentials with silicon-based electrodes. J Neurophysiol 2003;90:1314–23. [PubMed: 12904510]
14. Engstad T, Almkvist O, Viitanen M, Arnesen E. Impaired motor speed, visuospatial episodic memory and verbal fluency characterize cognition in long-term stroke survivors: the Tromso Study. Neuroepidemiology 2003;22:326–31. [PubMed: 14557682]
15. Ennaceur A, Delacour J. A new one-trial test for neurobiological studies of memory in rats. 1: Behavioral data. Behav Brain Res 1988;31:47–59. [PubMed: 3228475]
16. Ennaceur A, Meliani K. A new one-trial test for neurobiological studies of memory in rats. III. Spatial vs. non-spatial working memory. Behav Brain Res 1992;51:83–92. [PubMed: 1482548]
17. Feeney DM, Baron JC. Diaschisis. Stroke 1986;17:817–30. [PubMed: 3532434]
18. Fujita T, Yoshimine T, Maruno M, Hayakawa T. Cellular dynamics of macrophages and microglial cells in reaction to stab wounds in rat cerebral cortex. Acta Neurochir (Wien) 1998;140:275–9. [PubMed: 9638265]
19. Funkiewiez A, Ardouin C, Caputo E, Krack P, Fraix V, Klinger H, Chabardes S, Foote K, Benabid AL, Pollak P. Long term effects of bilateral subthalamic nucleus stimulation on cognitive function, mood, and behaviour in Parkinson's disease. J Neurol Neurosurg Psychiatry 2004;75:834–9. [PubMed: 15145995]
20. Gilman S, Dauth GW, Frey KA, Penney JB Jr. Experimental hemiplegia in the monkey: basal ganglia glucose activity during recovery. Ann Neurol 1987;22:370–6. [PubMed: 3674802]
21. Giordana MT, Attanasio A, Cavalla P, Migheli A, Vigliani MC, Schiffer D. Reactive cell proliferation and microglia following injury to the rat brain. Neuropathol Appl Neurobiol 1994;20:163–74. [PubMed: 8072646]
22. Hattori K, Lee H, Hurn PD, Crain BJ, Traystman RJ, DeVries AC. Cognitive deficits after focal cerebral ischemia in mice. Stroke 2000;31:1939–44. [PubMed: 10926961]
23. Hauss-Wegrzyniak B, Lynch MA, Vraniak PD, Wenk GL. Chronic brain inflammation results in cell loss in the entorhinal cortex and impaired LTP in perforant path-granule cell synapses. Exp Neurol 2002;176:336–41. [PubMed: 12359175]

24. Hauss-Wegrzyniak B, Vraniak PD, Wenk GL. LPS-induced neuroinflammatory effects do not recover with time. Neuroreport 2000;11:1759–63. [PubMed: 10852239]
25. Helmstaedter C, Van Roost D, Clusmann H, Urbach H, Elger CE, Schramm J. Collateral brain damage, a potential source of cognitive impairment after selective surgery for control of mesial temporal lobe epilepsy. J Neurol Neurosurg Psychiatry 2004;75:323–6. [PubMed: 14742620]
26. Hoofien D, Gilboa A, Vakil E, Donovick PJ. Traumatic brain injury (TBI) 10-20 years later: a comprehensive outcome study of psychiatric symptomatology, cognitive abilities and psychosocial functioning. Brain Inj 2001;15:189–209. [PubMed: 11260769]
27. Hovda DA, Lee SM, Smith ML, Von Stuck S, Bergsneider M, Kelly D, Shalmon E, Martin N, Caron M, Mazziotta J, et al. The neurochemical and metabolic cascade following brain injury: moving from animal models to man. J Neurotrauma 1995;12:903–6. [PubMed: 8594218]
28. Knoess C, Siegel S, Smith A, Newport D, Richerzhagen N, Winkeler A, Jacobs A, Goble RN, Graf R, Wienhard K, Heiss WD. Performance evaluation of the microPET R4 PET scanner for rodents. Eur J Nucl Med Mol Imaging 2003;30:737–47. [PubMed: 12536244]
29. Kossel AH, Williams CV, Schweizer M, Kater SB. Afferent innervation influences the development of dendritic branches and spines via both activity-dependent and non-activity-dependent mechanisms. J Neurosci 1997;17:6314–24. [PubMed: 9236241]
30. Moore TH, Osteen TL, Chatziioannou TF, Hovda DA, Cherry TR. Quantitative assessment of longitudinal metabolic changes in vivo after traumatic brain injury in the adult rat using FDG-microPET. J Cereb Blood Flow Metab 2000;20:1492–501. [PubMed: 11043912]
31. Mostafa RM, Mostafa YM, Ennaceur A. Effects of exposure to extremely low-frequency magnetic field of 2 G intensity on memory and corticosterone level in rats. Physiol Behav 2002;76:589–95. [PubMed: 12126997]
32. Paxinos, G.; Watson, C. The Rat Brain in Stereotaxic Coordinates. Academic Press; San Diego, CA: 1986.
33. Piot-Grosjean O, Wahl F, Gobbo O, Stutzmann JM. Assessment of sensorimotor and cognitive deficits induced by a moderate traumatic injury in the right parietal cortex of the rat. Neurobiol Dis 2001;8:1082–93. [PubMed: 11741403]
34. Polikov VS, Tresco PA, Reichert WM. Response of brain tissue to chronically implanted neural electrodes. J Neurosci Methods 2005;148:1–18. [PubMed: 16198003]
35. Rousche PJ, Pellinen DS, Pivin DP Jr, Williams JC, Vetter RJ, Kipke DR. Flexible polyimide-based intracortical electrode arrays with bioactive capability. IEEE Trans Biomed Eng 2001;48:361–71. [PubMed: 11327505]
36. Sanberg PR, Lehmann J, Fibiger HC. Impaired learning and memory after kainic acid lesions of the striatum: a behavioral model of Huntington's disease. Brain Research 1978;149:546–51. [PubMed: 27285]
37. Schiffer WK, Alexoff DL, Shea C, Logan J, Dewey SL. Development of a simultaneous PET/microdialysis method to identify the optimal dose of 11C-raclopride for small animal imaging. J Neurosci Methods 2005;144:25–34. [PubMed: 15848236]
38. Schiffer WK, Gerasimov MR, Bermel RA, Brodie JD, Dewey SL. Stereoselective inhibition of dopaminergic activity by gamma vinyl-GABA following a nicotine or cocaine challenge: a PET/microdialysis study. Life Sciences 2000;66:PL169–73. [PubMed: 10737423]
39. Schiffer WK, Mirrione MM, Biegon A, Alexoff DL, Patel V, Dewey SL. Serial microPET measures of the metabolic reaction to a microdialysis probe implant. J Neurosci Methods 2006;155:272–84. [PubMed: 16519945]
40. Schweinhardt P, Fransson P, Olson L, Spenger C, Andersson JL. A template for spatial normalisation of MR images of the rat brain. J Neurosci Methods 2003;129:105–13. [PubMed: 14511814]
41. Stensaas SS, Stensaas LJ. The reaction of the cerebral cortex to chronically implanted plastic needles. Acta Neuropathol (Berl) 1976;35:187–203. [PubMed: 782142]
42. Szarowski DH, Andersen MD, Retterer S, Spence AJ, Isaacson M, Craighead HG, Turner JN, Shain W. Brain responses to micro-machined silicon devices. Brain Res 2003;983:23–35. [PubMed: 12914963]

43. Tsabari, R.; Schiffer, WK.; Biegon, A. Society for Neuroscience. Washington, D.C.: 2005. Intracranial surgery results in long term changes in NMDA and perpheral benzodiazeping receptor density in rat brain. Program No. 950.12

44. Turner JN, Shain W, Szarowski DH, Andersen M, Martins S, Isaacson M, Craighead H. Cerebral astrocyte response to micromachined silicon implants. Exp Neurol 1999;156:33–49. [PubMed: 10192775]

45. Wagner KR, Kleinholz M, Myers RE. Delayed onset of neurologic deterioration following anoxia/ischemia coincides with appearance of impaired brain mitochondrial respiration and decreased cytochrome oxidase activity. J Cereb Blood Flow Metab 1990;10:417–23. [PubMed: 2158500]

46. Yoshino A, Hovda DA, Kawamata T, Katayama Y, Becker DP. Dynamic changes in local cerebral glucose utilization following cerebral conclusion in rats: evidence of a hyper-and subsequent hypometabolic state. Brain Res 1991;561:106–19. [PubMed: 1797338]

47. Yuen TG, Agnew WF. Histological evaluation of polyesterimide-insulated gold wires in brain. Biomaterials 1995;16:951–6. [PubMed: 8562785]

48. Zohar O, Schreiber S, Getslev V, Schwartz JP, Mullins PG, Pick CG. Closed-head minimal traumatic brain injury produces long-term cognitive deficits in mice. Neuroscience 2003;118:949–55. [PubMed: 12732240]

Abbreviations

PET
: Positron Emission Tomography

[^{18}F]FDG
: ^{18}F-fluorodeoxyglucose

NOR
: Novel Object Recognition

SPM
: Statistical Parametric Mapping

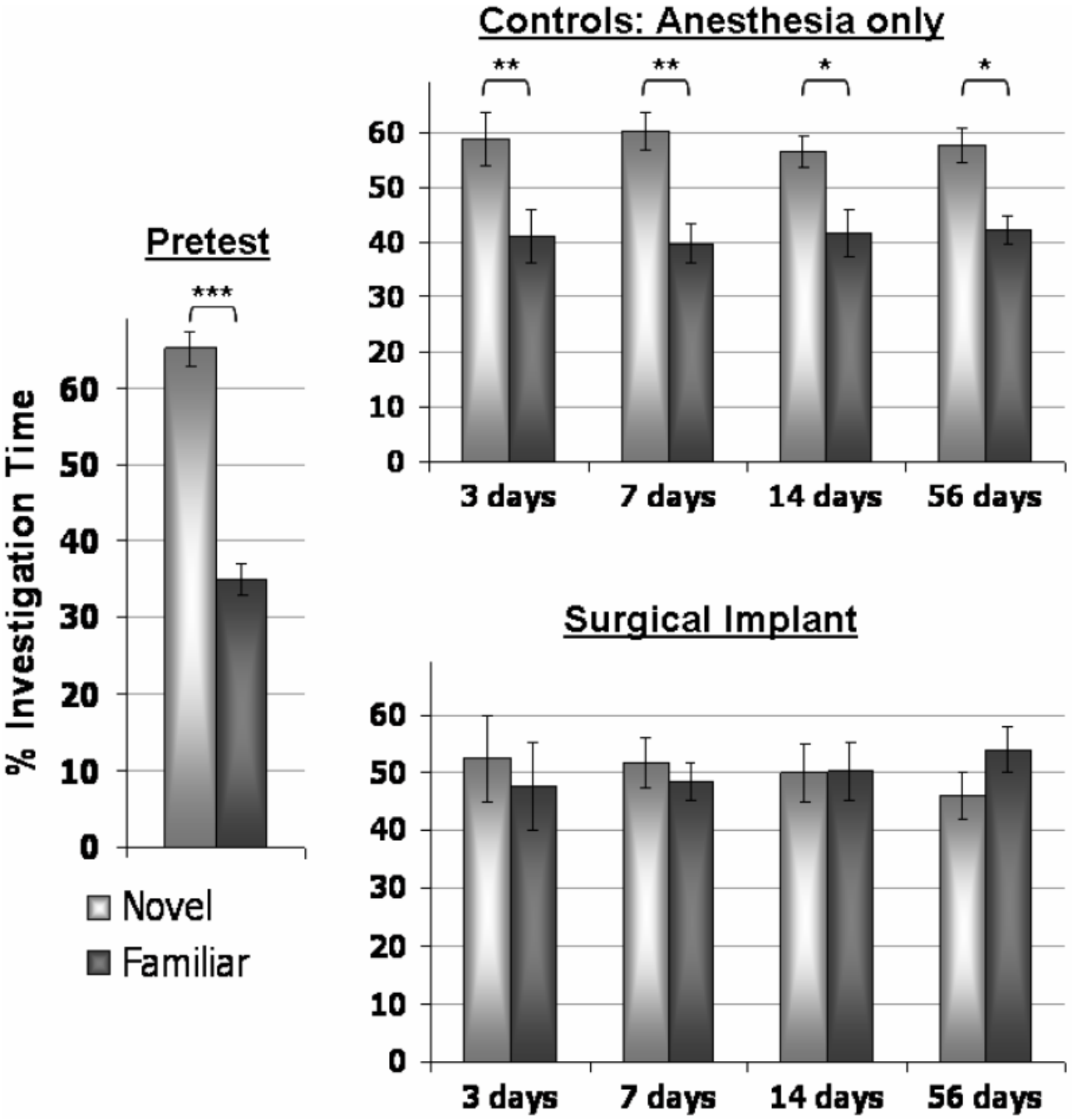

Figure 1. NOR performance for pre-and post-injury and control animals

Graphs depict percentage of total investigation time that animals investigated the familiar (dark grey) or the novel (light grey) object during each of the 5 minute test sessions. This percentage was calculated as the 'time at novel/total investigation time' and as 'time at familiar/total investigation time'. Bars indicate standard error of the mean (SEM). Significant differences in the duration of investigation at each object were determined with a two-tailed Student's t-test in which *$p<0.05$, **$p<0.01$ and ***$p<0.001$.

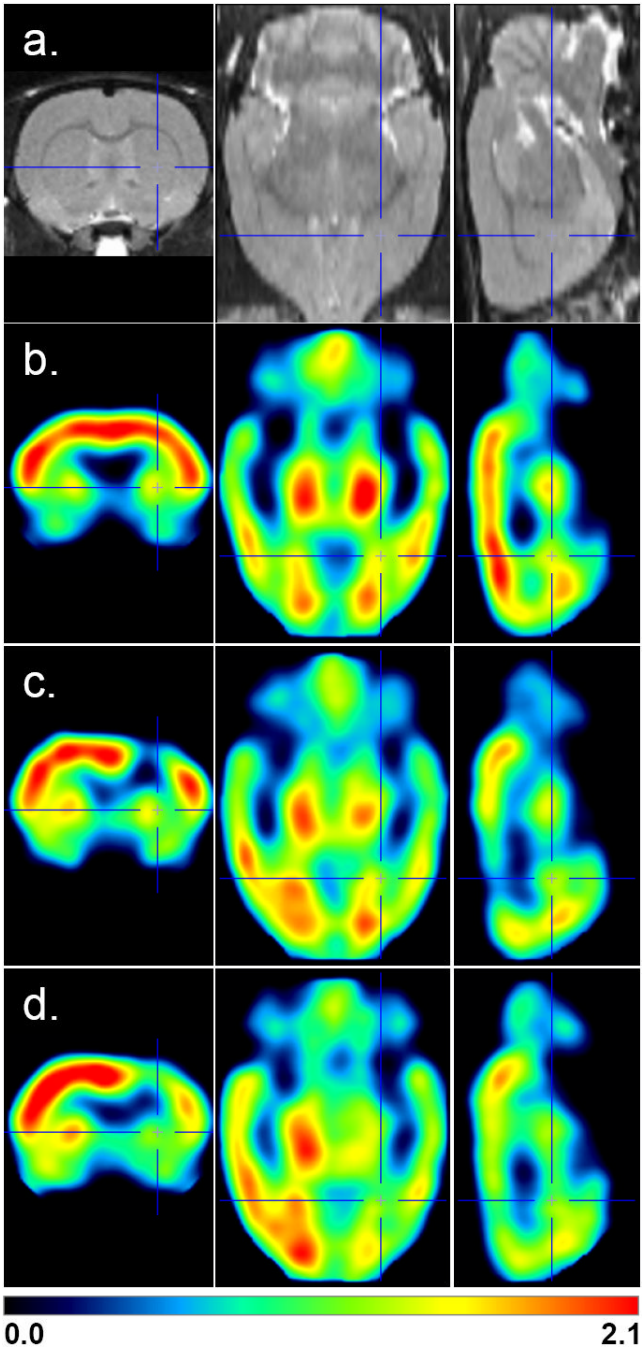

Figure 2. Serial FDG scans of animals with implants versus controls (mean images)

In (a), an MRI atlas is provided for anatomical detail. Control animals at the 28 day time point are shown in (b) while mean images from cannulated animals are shown at 28 days (c) and 58 days (c) after the surgery. Red shows regions with highest normalized uptake. Cross hairs indicate the target coordinates of the stereotaxic implant in Paxinos and Watson brain space, +2.5, +0.5, -6 mm x, y, z from the surface of the brain.

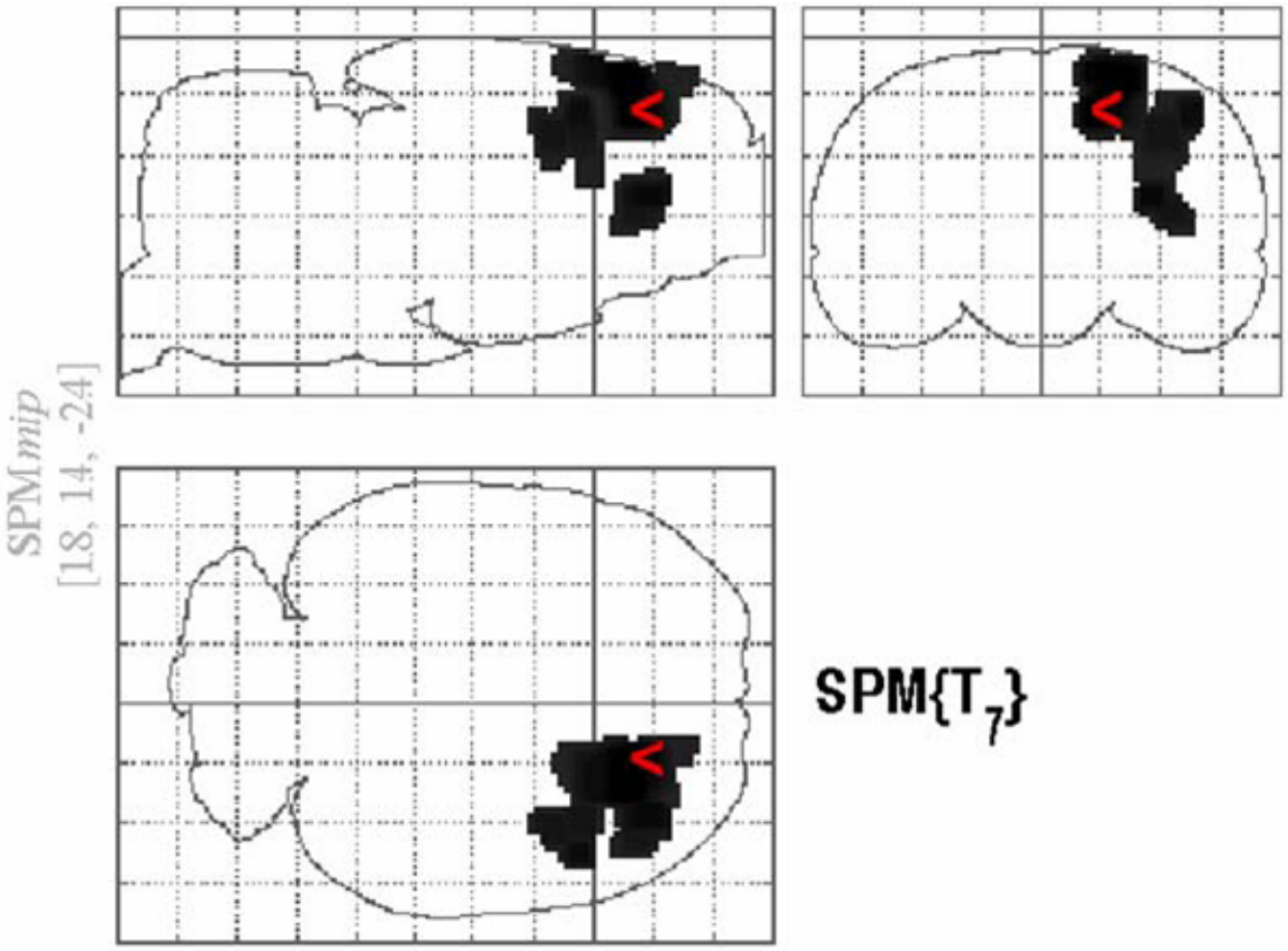

Figure 3. Glass–brain representation of the clusters with a significantly decreased [^{18}F]FDG accumulation in the surgical implant group as compared with the control group at 28 days after cannulation

Clusters were delineated from the SPM{T} map by a height threshold of T > 3.16 and by the threshold of cluster size over 100 contiguous voxels with the contrast of the control group minus the surgically implanted group.

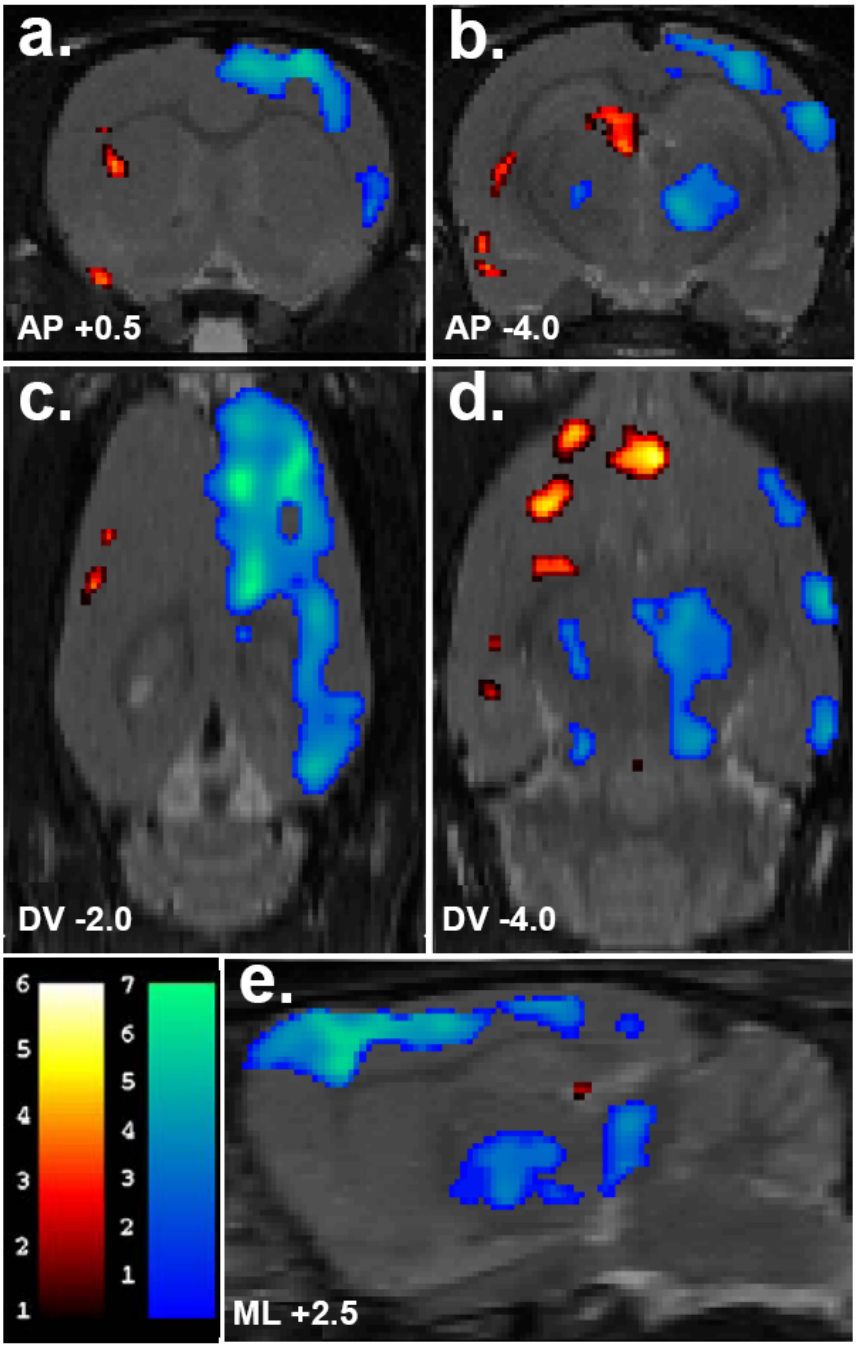

Figure 4. Changes in basal [^{18}F]FDG uptake 58 days following microdialysis probe implant targeting the right striatum

Numbers below the slices indicate their position relative to bregma in millimeters according to a standard rat brain atlas. Depicted in (a) and (b) are coronal slices (anterior-posterior coordinates, AP), in (c) and (d), transverse slices (dorsal-ventral coordinates, DV) and in (e), a sagittal slices (2.5 mm lateral to bregma). Colored overlays show statistically significant positive (red) and negative (blue) differences of animals with surgical implants (n=6) compared to controls (n=7). Significance is shown with a t-statistic color scale corresponding to the level of significance at the voxel level.

Table 1

Regional percent difference in resting [^{18}F]FDG uptake (left vs. right) at 28 and 58 days after surgical implant into the right striatum

Regions of interest (ROIs) were used to calculate hemisphere differences for controls (anesthesia only) or surgically implanted animals.

	Controls		Surgical Implants†	
Region	**Scan 1 (n=7) % Δ *(SEM)***	**Scan 2 (n=7) % Δ *(SEM)***	**Scan 1 (n=7) % Δ *(SEM)***	**Scan 2 (n=6) % Δ *(SEM)***
Frontal Cortex	2.04 *(1.78)*	3.47 *(1.02)*	-11.30 *(1.58)****	-13.71 *(2.69)****
Motor Cortex (M1)	1.05 *(0.92)*	-0.62 *(1.19)*	-24.65 *(4.83)****	-25.64 *(3.29)****
Sensory Cortex (S1)	-5.20 *(0.50)*	-5.26 *(0.82)*	-12.96 *(2.59)*	-17.04 *(3.15)***
Auditory Cortex	0.58 *(2.03)*	-1.31 *(0.92)*	-8.48 *(2.95)**	-9.25 *(3.23)*
Visual Cortex (V1-V2)	8.18 *(2.12)*	4.78 *(1.27)*	-5.63 *(3.52)****	-10.71 *(2.78)****
Caudate/Putamen	-3.94 *(1.34)*	-1.92 *(1.34)*	-8.85 *(2.89)*	-15.81 *(2.50)****
Thalamus	2.40 *(1.84)*	-0.13 *(0.94)*	-7.40 *(2.44)**	-9.98 *(1.68)**
Hippocampus	-3.53 *(3.22)*	-3.13 *(0.81)*	-5.12 *(0.67)*	-2.35 *(2.31)*
Colliculi (Superior)	-3.79 *(1.86)*	-3.57 *(1.40)*	-0.22 *(5.42)*	-3.66 *(2.60)*
Cerebellum	2.73 *(1.24)*	-3.43 *(2.52)*	-7.11 *(5.38)*	-0.26 *(1.96)*

† Comparisons were made between groups using a two-way ANOVA (region x group) followed by post-hoc Bonferroni analysis

* different from scan-specific control group, $p < 0.05$;

** different from scan-specific control group, $p < 0.01$;

*** different from scan-specific control group, $p < 0.001$

Table 2

Proportional time at novel vs. familiar objects in the subset of animals that received FDG scans.

Days post surgery	Control		Surgical	
	% time with novel Mean ± SEM	% time with familiar Mean ± SEM	% time with novel Mean ± SEM	% time with familiar Mean ± SEM
Presurgical	69 ± 5	31 ± 5	66 ± 3	34 ± 4
3	59 ± 5	41 ± 5	53 ± 5	47 ± 6
7	60 ± 3	40 ± 3	53 ± 4	47 ± 3
14	56 ± 3	42 ± 4	47 ± 5	53 ± 5
58	58 ± 3	42 ± 3	46 ± 4	54 ± 4